

Two-component controller design to safeguard data-driven predictive control

A tutorial to safe learning-based predictive control: exemplified with DeePC and Koopman MPC

Lea Bold*, Lukas Lanza*, Karl Worthmann*

Abstract. We design a two-component controller to achieve reference tracking with output constraints – exemplified on systems of relative degree two. One component is a data-driven or learning-based predictive controller, which uses data samples to learn a model and predict the future behavior of the system. We exemplify this component concisely by data-enabled predictive control (DeePC) and by model predictive control based on extended dynamic mode decomposition (EDMD). The second component is a model-free high-gain feedback controller, which ensures satisfaction of the output constraints if that cannot be guaranteed by the predictive controller. This may be the case, for example, if too little data has been collected for learning or no (sufficient) guarantees on the approximation accuracy derived. In particular, the reactive/adaptive feedback controller can be used to support the learning process by leading safely through the state space to collect suitable data, e.g., to ensure a sufficiently-small fill distance. Numerical examples are provided to illustrate the combination of EDMD-based model predictive control and a safeguarding feedback for the set-point transitions including the transition between the set points within prescribed bounds.

1 Introduction

Recently, there has been intensive research on data-driven methods in systems and control, see, e.g., the recent work [49]. In this note we focus on the control task of output tracking. For linear time-invariant (LTI) systems, the so-called fundamental lemma [77] by Jan C. Willems and coauthors paved the way for direct data-based predictive control, see, e.g., [21] (data-enabled predictive control, DeePC) for discrete-time LTI systems and also the recent survey [26] for extensions to stochastic LTI descriptor systems – provided that the collected input-output data is persistently exciting. The fundamental lemma has been further extended to, e.g., linear parameter-varying [73], flat [1], and continuous-

time systems [67]. Alternatives, suitable for nonlinear systems, are machine-learning methods. In particular, reinforcement learning (RL) has emerged as a particularly successful family of machine learning methods due to its close relationship to dynamic programming, see, e.g., [11, 37]. Despite its undeniable success, one of the main drawbacks is the comparatively-large data demand. Another, so-called indirect [24], technique using data-driven surrogate models for predictive control is based on the Koopman theory introduced in [41, 42]. Herein, the nonlinear system is first lifted using so-called observable functions, before the observables are propagated by the linear, but – in general – infinite-dimensional Koopman operator, see, e.g., the recent review article [19]. Using extended dynamic mode decomposition (EDMD; [39, 78]) a data-driven numerically-tractable approximation is computed. EDMD in the Koopman framework has been applied successfully in various examples, see, e.g., the textbook [52] as well as the references therein. Recently, this technique was successfully extended to control systems, see, e.g., [18] and [72] for linear and bilinear surrogate models, respectively. While linear surrogate models are attractive due to their simplicity, see, e.g., [43], the approximation accuracy is limited as recently shown in [17, 34]. A key advantage of Koopman-based methods is the available error analysis in the infinite-data limit [44], which was then further elaborated such that nowadays probabilistic finite-data error bounds exists for dynamical systems [54, 80] as well as their extension to stochastic and control systems [57], see also [61] for an extension to discrete- and continuous-time Markov processes on Polish spaces. Based on such error bounds, a Koopman-based (predictive) controller design with end-to-end guarantees can be achieved [13, 71]. However, uniform error bounds typically require invariance of the dictionary, i.e., the space spanned by finitely-many observables. While such assumptions may hold for autonomous systems relying on Koopman modes and eigenfunctions [34, 53, 55], the respective conditions [30] for control are more restrictive. Here, kernel EDMD [38, 62] provides a remedy, which even allows to rigorously establish Koopman invariance of the underlying reproducing kernel Hilbert space (RKHS) and, thus, to uniform error bounds [40]. Moreover, the respective techniques were

*Optimization-based Control Group, Institute of Mathematics, Technische Universität Ilmenau, Weimarer Straße 25, 98693 Ilmenau, Germany. E-mail: {lea.bold, lukas.lanza, karl.worthmann}@tu-ilmenau.de

Corresponding author: Lukas Lanza

recently extended to control-affine systems in [14].

To achieve such good tracking performances, all of the methods mentioned above rely on an offline training phase meaning that data have to be collected in advance. In this paper, we address this aspect. To ensure constraint satisfaction while taking advantage of learning control, the field of safe learning has gained importance and several safety frameworks have been proposed, see, e.g., the works [28, 33, 58] for concise overviews. To name but a few particular approaches, Hamilton-Jacobi equations and respective reachable sets are analyzed in [20], control barrier functions are utilized in [2], Lyapunov stability analysis results are used in [60] for RL, and safe learning in MPC is under consideration in [5]. Another approach that has attracted attention recently is the construction of so-called predictive safety filters. The idea is to test the controls using a model to ensure compliance with the prescribed conditions, cf. [74, 75] invoking barrier functions.

In this paper we use the idea of two-component controllers, cf. [69] or [3] for a tutorial introduction. The idea of combining two control strategies has already been applied successfully, e.g., for an event-based PI controller [66], combining feedforward open-loop control with feedback, as reported in [25] for a mechanical system, in [68] for continuous-time sampled-data systems in combination with DeePC using Willems et al.’s fundamental lemma, or in the superposition of RL-based controller and feedback [31, 36, 46] to name but a few. The two-component controller proposed in this paper is structurally similar to those in [31, 46] and consists of a learning-based predictive controller on the one hand, and the so-called funnel controller [10, 35] as a safeguarding reactive feedback controller on the other hand.

In the present paper we address the following two aspects of data-driven and learning-based control.

Achieve a prescribed fill distance. We apply the feedback controller with prescribed performance to the system and thereby make the system follow a pre-defined reference trajectory through the state space. This reference is chosen in such a way that the system visits desired pre-specified configurations, i.e., points in the state space, where samples are taken. If the reference is chosen such that the *fill distance* (see Definition 1) of system samples satisfies a predefined threshold, then, following the ideas in [14, 40] to approximate the Koopman operator using kernel EDMD, L^∞ -error bounds on the approximation error can be obtained.

Online learning predictive control. Safeguarded by the reactive feedback controller, a tracking task is started, and system data is collected during runtime, cf. Fig. 2. At some point, e.g., if a certain threshold for the fill distance is ensured or a certain amount of data is available, an EDMD surrogate model is computed and an EDMD-based predictive controller is activated. At this stage the reactive feedback controller intervenes only, if

the system enters a safety critical region, cf. Fig. 1b. Data collection is continued (and, potentially, the surrogate model is updated to improve its prediction capability) until, e.g. based on the fill distance, guarantees can be given using solely the predictive controller.

This paper is organized as follows. Section 2.1 introduces the system class under consideration and specifies the control objective. Section 2.2 presents our idea of designing a two-component controller; there, we describe the combination of *any* data-driven learning-based controller and the safeguarding outer-loop feedback controller, see Fig. 2. In Section 3 we briefly recall the concept of funnel control which is used to safeguard the overall controller. As a particular instance of a data-driven scheme, we discuss data-enabled predictive control (DeePC) in Section 4.1 and learning of the Koopman operator via Extended Dynamic Mode Decomposition (EDMD) in Section 4.2. To illustrate the proposed controller, we provide numerical simulations in Section 5.

Notation: $[n : m] = \mathbb{N}_0 \cap [n, m]$ for $n, m \in \mathbb{N}$ with $n \leq m$. $\langle \cdot, \cdot \rangle$ is the standard inner product on \mathbb{R}^n , $\|x\| := \sqrt{\langle x, x \rangle}$ for $x \in \mathbb{R}^n$; and for a symmetric positive definite matrix $Q \in \mathbb{R}^{n \times n}$ we write $\|x\|_Q := x^\top Q x$. For an interval $I \subset \mathbb{R}$, $C^p(I, \mathbb{R}^n)$ is the set of $p \in \mathbb{N}$ times continuously differentiable functions $f : I \rightarrow \mathbb{R}^n$, $L^\infty(I, \mathbb{R}^n)$ is the space of measurable essentially bounded functions $f : I \rightarrow \mathbb{R}^n$ with norm $\|f\|_\infty = \text{esssup}_{t \in I} \|f(t)\|$. $W^{k, \infty}(I, \mathbb{R}^n)$ is the Sobolev space of all k -times weakly differentiable functions $f : I \rightarrow \mathbb{R}^n$ with $f, \dots, f^{(k)} \in L^\infty(I, \mathbb{R}^n)$, and f_J denotes the restriction of f to $J \subset I$.

2 Two-component controller design for safe learning

In Section 2.1, we introduce the system class and define the control objective of output tracking within prescribed bounds. Then, in Section 2.2, we present the main idea, i.e., the design of the two-component controller, which enhances the performance of a safety-ensuring controller by combining it with a learning scheme. In this paper, we focus on funnel control to reliably ensure tracking within prescribed bounds and, then, use DeePC and EDMD to set up a surrogate model for predictive control to improve the closed-loop behavior.

2.1 System class and control objective

We assume that the system has the following form, which represents many mechanical systems without kinematic

constraints, see, e.g. [6],

$$\begin{aligned} \dot{x}_1(t) &= x_2(t), \\ \dot{x}_2(t) &= g_0(x_1(t), x_2(t)) + \sum_{i=1}^m g_i(x_1(t), x_2(t))u_i(t), \\ y(t) &= h(x_1(t), x_2(t)) = x_1(t), \end{aligned} \quad (1)$$

where $y(t) \in \mathbb{R}^m$ is the system's measured output and $u(t) = (u_1(t), \dots, u_m(t))^T \in \mathbb{R}^m$ denotes the control at time $t \in \mathbb{R}_{\geq 0}$; accordingly, $x(t) \in \mathbb{R}^{2m}$ is the state. The function $g_0 \in \mathcal{C}^1(\mathbb{R}^{2m}, \mathbb{R}^m)$ denotes the drift, and the maps $g_i \in \mathcal{C}^1(\mathbb{R}^{2m}, \mathbb{R}^m)$, $i \in [1 : m]$, distribute the input. For an input $u \in L_{\text{loc}}^\infty([0, \infty), \mathbb{R}^m)$ the (Carathéodory) solution $x(\cdot; \hat{x}, u)$ w.r.t. the initial condition $x(0; \hat{x}, u) = \hat{x}$ uniquely exists on its maximal interval of existence. We propose the following structural property on the system (1).

Assumption 1 (Known control direction). *The matrix-valued input distribution $G : \mathbb{R}^m \times \mathbb{R}^m \rightarrow \mathbb{R}^{m \times m}$ given by $(x_1, x_2) \mapsto [g_1(x_1, x_2), \dots, g_m(x_1, x_2)]$ is sign definite.*

In the following, we assume positive definiteness, i.e., $\langle z, G(x)z \rangle > 0$ for all $z \in \mathbb{R}^m \setminus \{0\}$ and all $x \in \mathbb{R}^{2m}$. This is not restrictive since negative definiteness will only change the sign in the feedback law (5).

For the output map $h(x) = x_1$, system (1) can be written as input-output dynamics

$$\begin{aligned} \ddot{y}(t) &= g_0(y(t), \dot{y}(t)) + \sum_{i=1}^m g_i(y(t), \dot{y}(t))u_i(t) \\ &= g_0(y(t), \dot{y}(t)) + G(y(t), \dot{y}(t))u(t), \end{aligned} \quad (2)$$

using G from Assumption 1.

Remark 1. While systems (2) are of order two, the proposed method can be extended to more general input-output systems of order $r \in \mathbb{N}$ of the form

$$\begin{aligned} y^{(r)}(t) &= f(t, \mathbf{T}(y, \dot{y}, \dots, y^{(r-1)})(t), u(t)), \\ y|_{[-b, 0]} &= y^0 \in C^{r-1}([-b, 0], \mathbb{R}^m), \end{aligned}$$

where $f \in \mathcal{C}(\mathbb{R}_{\geq 0} \times \mathbb{R}^\eta \times \mathbb{R}^m, \mathbb{R}^m)$ satisfies a so-called high-gain property, cf. [10, Def. 1.2], and the operator $\mathbf{T} : \mathcal{C}(\mathbb{R}_{\geq 0}, \mathbb{R}^m) \rightarrow L_{\text{loc}}(\mathbb{R}_{\geq 0}, \mathbb{R}^\eta)$ satisfying [10, Def. 1.1] models bounded though unobservable internal dynamics, hysteresis effects and delays. However, for the sake of clarity, we restrict the presentation to systems (1), respectively (2). \diamond

The control objective is that the output y of system (1) follows a given reference trajectory $y_{\text{ref}} \in W^{2,\infty}([0, \infty), \mathbb{R}^m)$ within predefined error margins for all times. The latter means that the tracking error $e(t) := y(t) - y_{\text{ref}}(t)$ satisfies

$$\|y(t) - y_{\text{ref}}(t)\| < 1/\sigma(t) \quad \forall t \geq 0, \quad (3)$$

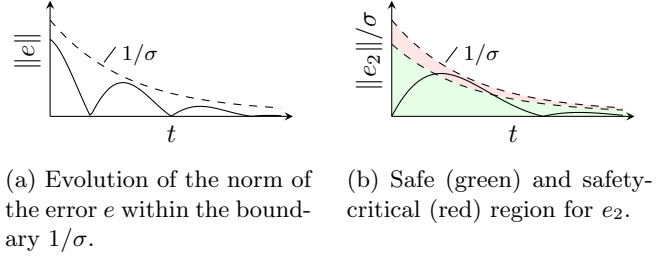


Figure 1: Schematic illustration of tracking error, funnel boundary as well as safe and safety-critical areas [31].

where σ is a time-varying error margin chosen by the control engineer, which belongs to the set

$$\Sigma := \{\sigma \in W^{1,\infty}([0, \infty), \mathbb{R}) \mid \inf_{s \geq 0} \sigma(s) > 0\}.$$

The control objective (3) is depicted in Fig. 1a.

2.2 Two-component controller

To achieve the control objective (3), we propose a two-component controller combining a data-driven learning-based controller and a safeguarding feedback controller, cf. Fig. 2. To improve performance, the data-driven con-

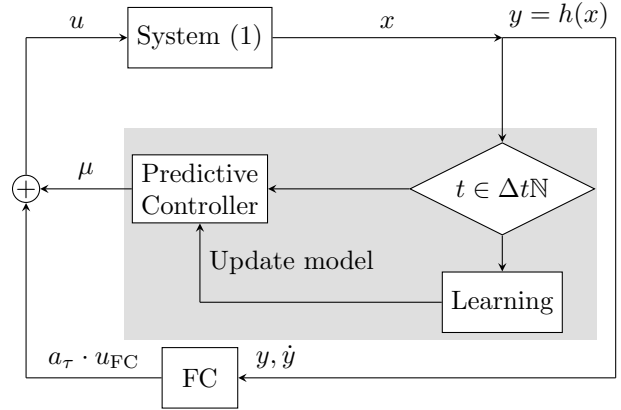


Figure 2: Structure of the two-component controller. The data-driven learning-based *Predictive Controller* in the gray box is safeguarded by the *Funnel Controller*. To limit activity of the latter, the input u_{FC} is multiplied by the activation function a_τ . For brevity, the reference y_{ref} is not shown explicitly but it is provided to both controller components.

troller is typically assumed to be of predictive type (e.g. MPC, DeePC, Subspace Predictive Control). However, a combination with other reactive feedback controllers, e.g. learning the gain from data [22, 23], is also possible.

We denote the control signal from the data-driven (predictive) controller by μ , and the safeguarding control signal by u_{FC} . The combination of both control signals μ and u_{FC} is used to achieve the control objective (3). A

straight forward combination would be

$$u = \mu(t, x) + u_{\text{FC}}(t).$$

With this, however, the safeguarding outer-loop funnel controller would interrupt the predictive controller whenever an auxiliary error variable is non-zero. Hence, we introduce an activation function similar to event-triggered control, see, e.g., [47, 48, 64]. Following the ideas in [31], we introduce for a dwell-time $\tau > 0$ and an activation threshold λ an activation function $a_\tau(t, e(t), \dot{e}(t))$, see (6) for details. The activation threshold separates the “safe” and “safety-critical” region in the output space (more precise in the tracking-error space), cf. Fig. 1b. Only if the auxiliary signal leaves the safe λ -region, the funnel controller contributes to the control signal. Since the funnel controller may instantaneously push the auxiliary variable back into the safe region, the dwell-time $\tau > 0$ is incorporated to avoid chattering. For an activation function $a_\tau(t, e(t), \dot{e}(t))$, we define the overall control signal

$$u(t) = \mu(t, x) + a_\tau(t, e(t), \dot{e}(t)) u_{\text{FC}}(t). \quad (4)$$

To give an idea, how the controller works, we follow the signals in Fig. 2, omitting the time argument. Note that (as usual) we design the controller assuming that the prediction step in the data-driven controller (e.g. finite horizon optimal control problem in MPC) is solved instantaneously. This means that at $t = k\Delta t$, where $\Delta t > 0$ is the sampling time, the current state $x(k\Delta t)$ is given to the prediction scheme which calculates the control input $\mu : [k\Delta t, (k+N)\Delta t) \rightarrow \mathbb{R}^m$. Here, $k \in \mathbb{N}$ is the sampling instance, and $N \in \mathbb{N}$ is the prediction horizon, cf. Algorithm 1. We may assume that for the learning scheme the system state x is available. If $t = k\Delta t$, then the data $x(k\Delta t)$ is given to the learning entity. Given the data $x(0), \dots, x(d\Delta t)$ (for some amount of data $d > 0$) and the recorded input u , the learning entity supplies, e.g., a model that explains the data best (w.r.t certain criteria). This model is handed over to the predictive controller. Note that the model is not necessarily updated every Δt . The updates can (and will) be made after arbitrary sampling instances. Based on the (updated) model the predictive controller produces (e.g. via finite horizon optimal control) a control signal μ , which is handed over to an adder. For the funnel controller we take y, \dot{y} from the system, and $y_{\text{ref}}, \dot{y}_{\text{ref}}$ is given. These signals are handed over to the funnel controller computing u_{FC} . Based on the current error and its derivative, the control signal u_{FC} is active or inactive by multiplication with a_τ . Therefore, the resulting control input is $u = \mu + a_\tau u_{\text{FC}}$. Note that since the funnel controller receives the signals y, \dot{y} continuously, the signal u_{FC} implicitly depends on the signal $\mu(t, x)$ through the closed-loop continuous-time dynamics (1), (4).

3 Safeguarding mechanism

As the safeguarding controller component we utilize a high-gain adaptive feedback law. In the present paper we use *funnel control*, first proposed in [35], but recognize that for the system class under consideration we could have used the *prescribed performance control* methodology [7, 8] as well. Both controllers are suitable to achieve (3) for systems (1). Let a prescribed tolerance $\sigma \in \Sigma$ be given. Then, for system (1) satisfying Assumption 1, a funnel control feedback law is given in the simple form, cf. [10],

$$\begin{aligned} e_1(t, y(t)) &:= \sigma(t)e(t) = \sigma(t)(y(t) - y_{\text{ref}}(t)), \\ e_2(t, y(t), \dot{y}(t)) &:= \sigma(t)\dot{e}(t) + \frac{e_1(t)}{1 - \|e_1(t)\|^2}, \\ u_{\text{FC}}(t, y(t), \dot{y}(t)) &:= -\frac{e_2(t)}{1 - \|e_2(t)\|^2}, \end{aligned} \quad (5)$$

where we omit the precise definition of the domain of e_1, e_2 , respectively. To avoid confusion with the discrete-time setting for EDMD presented in Section 4.2.1, we explicitly state the following assumption.

Assumption 2 (Availability of signals). *The signals $y(t), \dot{y}(t), y_{\text{ref}}(t)$ and $\dot{y}_{\text{ref}}(t)$ are continuously available to the controller (5).*

We emphasize the particular feature of funnel control that no system parameters are involved in the feedback law (5), i.e., it is model-free.

Next, we make the notion of the activation function mentioned in Section 2.2 precise. Let $\lambda \in (0, 1)$ and use the error variables defined in (5). We specify the activation function $a_\tau : \mathbb{R}_{\geq 0} \times \mathbb{R}^m \rightarrow [0, 1]$ as follows

$$a_\tau(t, e_2(t)) = \max\{0, \max_{s \in [t-\tau, t]} \|e_2(s)\| - \lambda\}. \quad (6)$$

The activation function has two parameters $\lambda \in (0, 1)$ and $\tau > 0$. The activation threshold λ determines the safe region within the funnel boundaries, cf. Fig. 1b. For small values of λ the funnel controller intervenes already for small deviations from the reference. For λ close to 1 the funnel controller reacts late which results in high peaks of the control input since the feedback has to push back the error rapidly. The latter is, in particular, relevant when performing numerical simulations. The parameter $\tau > 0$ defines the dwell-time to avoid chattering when e_2 leaves the λ -region. Large values of $\tau > 0$ keep the funnel controller active for a long time even if e_2 is already in the safe region which may have effects on the prediction based controller. The more reliable the predictive controller is, the smaller the dwell-time τ can be chosen. Note that, since $e_2 = e_2(t, y, \dot{y})$, the above definition of a_τ is in line with the previous informal introduction, where we used $a_\tau(t, e(t), \dot{e}(t))$. To save on

notation, we use $a_\tau(t, e_2)$ in the following. As a first result we record the following safeguarding property. It combines – with minor changes – the idea of using an activation function as in [9] with the observations shown in [31, Thm. 1]. The feasibility proof mainly relies on the proof of [10, Thm. 1.9], and the insights in [46, Thm. 5.1] for sampled-data systems.

Theorem 1 (Safeguarding property). *Consider a system (1). Let a reference trajectory $y_{\text{ref}} \in W^{2,\infty}(\mathbb{R}_{\geq 0}, \mathbb{R}^m)$ and a funnel function $\sigma \in \Sigma$ be given. If Assumptions 1 and 2 are satisfied and for the auxiliary variables in (5) it holds*

$$\|e_1(0)\| < 1 \text{ and } \|e_2(0)\| < 1,$$

then any solution of the closed loop system (1), (4) satisfies $\|y(t) - y_{\text{ref}}(t)\| < 1/\sigma(t)$ for all $t \geq 0$, i.e., the control objective (3) is satisfied, where $\mu(\cdot)$ is a bounded input generated by the predictive controller, and $a_\tau(\cdot) u_{\text{FC}}(\cdot)$ is given by (5), (6).

Main ideas of the proof. We omit the technical details here and justify the result by following the reasoning given in [31, Thm. 1] instead. The input signal $\mu(\cdot)$ generated by the prediction-based controller is bounded. For $\lambda \in (0, 1)$ from (6) and invoking Assumptions 1 and 2 it can be shown by contradiction that there exists $\tilde{\varepsilon} \in [\lambda, 1)$ such that $\|e_i(t)\| \leq \tilde{\varepsilon}$ for all $t \geq 0$, and $i = 1, 2$. The respective analysis can be restricted to time intervals, where $\|e_2(t)\| \in [\lambda, 1)$ (red area in Fig. 1b). In these intervals, the analysis in the proof of [10, Thm. 1.9] applies. Therefore, multiplying u_{FC} by α_τ , which is potentially zero, does not jeopardize the analysis in the safety-critical zone, meaning that we can employ the same line of arguments as in [10, 31, 46]. \diamond

Note that Theorem 1 means that the proposed two-component controller design can be used for safe learning during runtime, more precisely, to perform safe learning-based predictive control without offline training, since constraints satisfaction in the output is guaranteed by the safeguarding feedback controller. This is illustrated by a numerical simulation in Section 5.

4 Data-based control

In this section, we present two instances of a two-component controller. In Section 4.1, we recap Willems and coauthors' fundamental lemma [77] and its use for predictive control of linear time-invariant systems following [21]. Hereby, we leverage our previous works [46, 68]. Then, we present recent results for nonlinear systems using the Koopman operator in Section 4.2.

4.1 Data-enabled predictive control

Consider the discrete-time LTI system

$$x^+ = Ax + Bu, \quad y = Cx, \quad (7)$$

with output $y \in \mathbb{R}^m$, where according to system class (1) and Assumption 1

$$A = \begin{bmatrix} 0 & I \\ A_1 & A_2 \end{bmatrix}, \quad B = \begin{bmatrix} 0 \\ B_1 \end{bmatrix}, \quad C = [I_m \quad 0]$$

for $A_1, A_2 \in \mathbb{R}^{m \times m}$, and positive definite $B_1 \in \mathbb{R}^{m \times m}$. Therefore, system (7) is minimal, i.e., controllable and observable. To recap DeePC [21], we first recall the concept of persistently exciting signals and a statement for systems (7). For $1 \leq d \in \mathbb{N}$ a real sequence $(u_k)_{k=0}^{d-1}$ is called persistently exciting of order $L \in \mathbb{N}$ if the so-called Hankel matrix

$$\mathcal{H}_L(u_{[0,d-1]}) = \begin{bmatrix} u_0 & u_1 & \dots & u_{d-L} \\ u_1 & u_2 & \dots & u_{d-L+1} \\ \vdots & \vdots & \ddots & \vdots \\ u_{L-1} & u_L & \dots & u_{d-1} \end{bmatrix}$$

has full row rank. Given a persistently exciting input, the following result can be shown for systems (7) known as the fundamental lemma [77]; slightly simplified for the current purpose.

Lemma 1 ([77]). *Let $((\hat{u}_k)_{k=0}^{d-1}, (\hat{y}_k)_{k=0}^{d-1})$ be input-output data of (7), where the input $(\hat{u}_k)_{k=0}^{d-1}$ is persistently exciting of order $L + 2m$. Then $((u_k)_{k=0}^{L-1}, (y_k)_{k=0}^{L-1})$ is an input-output trajectory of (7) of length L if and only if there exists $\nu \in \mathbb{R}^{d-L+1}$ such that*

$$\begin{bmatrix} u_{[0,L-1]} \\ y_{[0,L-1]} \end{bmatrix} = \begin{bmatrix} \mathcal{H}_L(\hat{u}_{[0,d-1]}) \\ \mathcal{H}_L(\hat{y}_{[0,d-1]}) \end{bmatrix} \nu.$$

This representation can be used to set up a purely data-driven predictive controller to make the output of system (7) track a reference trajectory given by $(y_{\text{ref}}(k))_{k=0}^\infty$, while – like in MPC – satisfying input constraints. Assume that for a prediction horizon $N > 0$ the input-output data $((\hat{u}_k)_{k=0}^{d-1}, (\hat{y}_k)_{k=0}^{d-1})$ of system (7) is given and that the input data $(\hat{u}_k)_{k=0}^{d-1}$ is persistently exciting of order $N + 4m$. In every discrete time step $k \in \mathbb{N}$ the optimal control problem to be solved is given by (here and later we use quadratic stage costs costs to keep the presentation simple)

$$\underset{(u,y,\nu)}{\text{minimize}} \quad \sum_{i=k+1}^{k+N} \left(\|y(i) - y_{\text{ref}}(i)\|_Q^2 + \|u(i)\|_R^2 \right) \quad (8a)$$

with $(u, y) = ((u(i))_{i=k-2m+1}^{k+N}, (y(i))_{i=k-2m+1}^{k+N})$ subject to

$$\begin{bmatrix} u_{[k-2m+1,k+N]} \\ y_{[k-2m+1,k+N]} \end{bmatrix} = \begin{bmatrix} H_{N+2m}(\hat{u}) \\ H_{N+2m}(\hat{y}) \end{bmatrix} \nu, \quad (8b)$$

$$\begin{bmatrix} u_{[k-2m+1,k]} \\ y_{[k-2m+1,k]} \end{bmatrix} = \begin{bmatrix} \tilde{u}_{[k-2m+1,k]} \\ \tilde{y}_{[k-2m+1,k]} \end{bmatrix}, \quad (8c)$$

$$\|u(i)\| \leq u_{\text{max}}, \quad i = k+1, \dots, k+N.$$

Here, $Q, R \in \mathbb{R}^{m \times m}$ in (8a) are symmetric positive definite weighting matrices. The past input-output trajectory is denoted by $(\tilde{u}, \tilde{y}) = ((\tilde{u}(i))_{i=k-2m+1}^k, (\tilde{y}(i))_{i=k-2m+1}^k)$, and in combination with the observability of (7) the constraint (8c) serves as initial condition such that the trajectory is continued. The main difference to model predictive control is that in the optimal control problem (8) the state-space model (7) is replaced by the non-parametric description (8b) based on Lemma 1.

For the sake of clear presentation let us denote the control generated by (8) by u_{DPC} , and $u_{\text{DPC}}(t) = u_{\text{DPC}}(k)$ for $t \in [k, k+1)$. According to the idea presented in Section 2.2 the overall input reads

$$u(t) = u_{\text{DPC}}(t) + a_r(t, e_2)u_{\text{FC}}(t).$$

Since Theorem 1 ensures satisfaction of the control objective (3), the data required to set up the Hankel matrices (8b) can be collected during runtime without offline training. Numerical results for the combination of the data-driven scheme (8) with a (sampled-time) funnel controller are presented in [46, 68], where also adaption of the prediction horizon based on the available data is discussed.

4.2 Koopman-based control

Although there exist results extending the techniques based on the fundamental lemma to, e.g., linear parameter-varying [73], flat [1], and continuous-time systems [67], in its roots this technique is restricted to linear systems. Now, due to its ability to handle nonlinear systems, we utilize MPC based on an EDMD surrogate model in the prediction step, see, e.g., [13, 43] as a second particular instance for the learning-based predictive control component (gray box in Fig. 2). Thereby, we take advantage of recently-derived finite-data pointwise error bounds for control systems [14].

4.2.1 Extended Dynamic Mode Decomposition

First, we briefly recap the basic idea of extended dynamic mode decomposition (EDMD). To this end, we consider a discrete-time system

$$x^+ = F(x) \quad (9)$$

with continuous nonlinear map $F : \mathbb{R}^n \rightarrow \mathbb{R}^n$. Then the Koopman operator is defined by the identity

$$(\mathcal{K}\varphi)(\tilde{x}) = \varphi(F(\tilde{x}))$$

for all $\tilde{x} \in \mathbb{R}^n$, and functions $\varphi : \mathbb{R}^n \rightarrow \mathbb{R}$, the so-called observables. The Koopman operator \mathcal{K} is a bounded linear operator on a suitably-defined space of observable functions φ . However, the Koopman operator is, in general, infinite dimensional.

EDMD is a data-based learning method to approximate the compression $P_{\mathbb{V}}\mathcal{K}|_{\mathbb{V}}$ of the Koopman operator on the compact set $\mathbb{X} \subset \mathbb{R}^n$, see, e.g., [57, 78] for details. Therein, the space $\mathbb{V} := \text{span}\{\psi_j\}_{j=0}^M$ is spanned by finitely many observables. Let $\Psi = (\psi_0, \psi_1, \dots, \psi_M)^\top$ be the vector of all observables with $\psi_0 \equiv 1$ and $\psi_j \in \mathcal{C}^1(\mathbb{R}^n, \mathbb{R})$ for all $j \in [1 : M]$ such that $\Psi : \mathbb{R}^n \rightarrow \mathbb{R}^{M+1}$. Then, for randomly i.i.d. sampled data pairs $(x_i, F(x_i))$, $i \in [1 : d]$, the operator $P_{\mathbb{V}}\mathcal{K}|_{\mathbb{V}}$ is approximated by a linear map, which we represent by a matrix $K = K_d^M \in \mathbb{R}^{(M+1) \times (M+1)}$, where d refers to the number of data points. To this end, the regression problem

$$K = \underset{\hat{K} \in \mathbb{R}^{(M+1) \times (M+1)}}{\text{argmin}} \|\Psi_{X^+} - \hat{K}\Psi_X\|_F$$

is solved with data matrices $\Psi_X := [\Psi(x_1) \dots \Psi(x_d)]$ and $\Psi_{X^+} := [\Psi(F(x_1)) \dots \Psi(F(x_d))]$. Using the pseudo-inverse, the solution reads $K = \Psi_{X^+}\Psi_X^\dagger$. Based on this approximation in the lifted space \mathbb{V} and assuming full rank of the lift Ψ , an EDMD-based surrogate model of system (9) can be defined by $x^+ = P_{\mathbb{X}}K\Psi(x)$, where $P_{\mathbb{X}}$ is the orthogonal projection on the state space. To simplify the *projection back* onto the state space [50, 51], we assume that the coordinate functions are observables, i.e., $\psi_i(x) = e_i^\top x$ for $i \in [1 : n]$, where e_i denotes the i -th unit vector, and refer to [29] for more-sophisticated re-projection techniques. Then, using the simple *coordinate re-projection* yields the surrogate model

$$x^+ = \begin{bmatrix} I_n & 0_{n \times m} \end{bmatrix} K\Psi(x). \quad (10)$$

Remark 2. If the underlying dynamics are governed by a continuous-time dynamical system $\dot{x}(t) = f(x(t))$ with locally Lipschitz-continuous map $f : \mathbb{X} \rightarrow \mathbb{R}^n$, the corresponding discrete-time system is given by

$$x^+ = F(\tilde{x}) := \tilde{x} + \int_0^{\Delta t} f(x(s; \tilde{x})) ds$$

for a fixed time step $\Delta t > 0$, where $x(\cdot; \tilde{x})$ represents the solution of the (ordinary) differential equation satisfying the initial condition $x(0; \tilde{x}) = \tilde{x}$.

4.2.2 EDMD-based predicted control

Next, we briefly recap an extension of the presented approximation technique EDMD to nonlinear control-affine systems. There are different approaches to incorporate inputs, e.g., *EDMD with control* (EDMDc) corresponding to a linear data-driven surrogate model [43, 63], or the recently proposed method in [4] for systems (1), where the input enters linearly. Here, we proceed with a bilinear model, see, e.g., [59, 72] and the references therein. The reasoning behind is twofold. On the one hand, the authors of [34] clearly point out structural limitations of linear surrogate models due to the imposed decoupling of (lifted) state and control. On the other hand, they proposed LPV systems as a remedy pointing

out that bilinear models suffice if the dynamics of the original system are control affine. To this end, the key insight is that the Koopman generator, which generates the semigroup $(\mathcal{K}^t)_{t \geq 0}$ of linear Koopman operators, preserves control affinity. This property is approximately preserved for the Koopman operator for sampled-data systems with zero-order hold, i.e.,

$$x^+ = \tilde{x} + \int_0^{\Delta t} g_0(x(s; \tilde{x}, u)) ds + \sum_{i=1}^m \tilde{u}_i \int_0^{\Delta t} g_i(x(s; \tilde{x}, u)) ds$$

with $u(s) \equiv \tilde{u} \in \mathbb{R}^m$, and results in an additional error of magnitude $\mathcal{O}(\Delta t^2)$, see [14, Rem. 4.2] for details. Overall, using the approximate control affinity analogously to [57, 59], we obtain the bilinear EDMD surrogate

$$x^+ = \hat{F}(x, u) = \begin{bmatrix} I_n & 0_{n \times m} \end{bmatrix} K_u^{\Delta t} \Psi(x) \quad (11)$$

to approximate the Koopman operator $\mathcal{K}_u^{\Delta t}$ for $u \in \mathbb{R}^m$ using the decomposition

$$K_u^{\Delta t} = K_0^{\Delta t} + \sum_{i=1}^m u_i (K_i^{\Delta t} - K_0^{\Delta t}),$$

where $K_0^{\Delta t}$ corresponds to $\tilde{u} = 0$ and $K_i^{\Delta t}$ to $\tilde{u} = e_i$, $i \in [1 : m]$. Koopman-based surrogate models can be used to perform model predictive control based on system data, as shown, e.g., in [43] for EDMDc or with the previously introduced methodology resulting in a bilinear surrogate (11), in [13, 27, 56, 65] to name a few. The underlying idea is to perform predictions for the observables satisfying the discrete-time dynamics (11). In the following, $\bar{x}_{\bar{u}}(\kappa, \hat{x})$ denotes the predicted trajectory emanating from state \hat{x} at time κ , $\kappa \in [0 : N]$, if the sequence of control values $(\bar{u}(\kappa))_{\kappa=0}^{N-1}$ is applied. To keep the presentation technically simple, we use the quadratic stage costs $\ell : \mathbb{N}_0 \times \mathbb{R}^n \times \mathbb{R}^m \rightarrow \mathbb{R}_{\geq 0}$ defined by

$$\ell(k, x, u) := \|x - x_{\text{ref}}(k\Delta t)\|_Q^2 + \|u\|_R^2$$

with symmetric and positive definite matrices $Q \in \mathbb{R}^{n \times n}$ and $R \in \mathbb{R}^{m \times m}$. An EDMD-based MPC scheme is presented in Algorithm 1.

It has been shown in [13] that under suitable assumptions Algorithm 1 defines a practical asymptotically stabilizing controller for nonlinear systems (1) using finite-data error bounds, cost controllability, and a sufficiently long prediction horizon, see [32] and [12].

Remark 3. Note that the EDMD procedure relies on piecewise constant control inputs $u(t) \equiv u_k$ for $t \in [k\Delta t, (k+1)\Delta t)$. Therefore, to obtain reasonable data to learn from, collected during runtime, the data collection can be equipped with a post-processing condition. One possibility is to apply u_k for $t \in [k\Delta t, (k+1)\Delta t)$ and evaluate whether the funnel controller was active in this interval or not by considering the activation function in (6). If $\alpha_\tau(t, e_2(t)) = 0$ for all $t \in [k\Delta t, (k+1)\Delta t)$, then the data can be used for learning. \diamond

Algorithm 1 EDMD-based MPC

Input: Time instant $k \in \mathbb{N}_0$, prediction horizon $N \in \mathbb{N}_{\geq 2}$, time shift $\Delta t > 0$

1. At time instant $k \in \mathbb{N}_0$ measure $\hat{x} = x(k\Delta t)$ and receive the reference $(x_{\text{ref}}(\kappa))_{\kappa=k}^{k+N}$
2. Solve the optimization problem

$$\begin{aligned} & \underset{\bar{u}=(\bar{u}(\kappa))_{\kappa=0}^{N-1}}{\text{minimize}} && \sum_{\kappa=0}^{N-1} \ell(k + \kappa, \bar{x}_{\bar{u}}(\kappa, \hat{x}), \bar{u}(\kappa)) \\ & \text{subject to} && \bar{x}_{\bar{u}}(\kappa + 1, \hat{x}) = \hat{F}(\bar{x}_{\bar{u}}(\kappa, \hat{x}), \bar{u}(\kappa)), \\ & && \bar{u}(\kappa) \in \mathbb{U}, \quad \forall \kappa \in [0 : N - 1], \end{aligned}$$

to compute a minimizing sequence $\bar{u}^* := (\bar{u}^*(\kappa))_{\kappa=0}^{N-1}$ of control values

3. Apply feedback value $\mu_{\text{MPC}}(k, x(k\Delta t)) = \bar{u}^*(0)$, set $k \leftarrow k + 1$, and go to step 1
-

As shown e.g. in [15] a key challenge for successive application of EDMD and EDMD-based MPC is the choice of the observable functions constituting the dictionary that spans the subspace \mathbb{V} where the Koopman operator is approximated on. The selection and construction of dictionaries that suit the underlying system is discussed e.g. in [45]. In the next section we concisely recap kernel-based EDMD, see [79], which attends to the aspect of choosing a dictionary. In these works, the dictionary is constructed from kernels, which are defined through the available data points.

4.2.3 Sampling and approximation error

Performing any kind of approximate identification or learning of dynamics from data, the question naturally arises as to how good the approximation is. In recent years this question has been addressed intensively in the context of the Koopman framework. The bounds on the approximation error of the Koopman operator/generator are typically provided as probabilistic statements, see [54, 61, 80] and the references therein. In particular, the error bounds are derived on the assumption of either i.i.d. or ergodic sampling. However, in practice it is difficult to meet the requirements for i.i.d. or ergodic sampling. This issue can be avoided by using kernel-EDMD to approximate autonomous dynamics using the canonical features as observables in a suitably-chosen reproducing kernel Hilbert space (RKHS). Moreover, the respective error bounds provide pointwise bounds exploiting the so-called reproducing property and Koopman invariance of the underlying RKHS, see [40]. Then, the results were extended in [14] to control systems, where, in addition, proportional error bounds w.r.t. the fill distance of data samples were established. The fill distance $h_{\mathcal{X}}$ corresponds to the radius of the largest ball with center in \mathbb{X} , which has no intersection with the set of samples \mathcal{X} .

Definition 1 (Fill distance $h_{\mathcal{X}}$). For a bounded set $\mathbb{X} \subset \mathbb{R}^n$ and a set of samples $\mathcal{X} := \bigcup_{i=1}^d \{x_i\} \subset \mathbb{X}$, $d \in \mathbb{N}$, the fill distance $h_{\mathcal{X}}$ w.r.t. \mathbb{X} is defined by

$$h_{\mathcal{X}} := \sup_{x \in \mathbb{X}} \min_{x_i \in \mathcal{X}} \|x - x_i\|.$$

The first uniform bound for the full approximation error for kernel EDMD (kEDMD) was derived in [40] using the RKHS generated by Wendland kernel functions, see [76]. We recall the result (in a slightly-simplified fashion) in the following theorem.

Theorem 2 (Theorem 5.2 of [40]). Let the bounded set $\mathbb{X} \subset \mathbb{R}^n$ have Lipschitz boundary. Further, let \mathbb{H} be the RKHS generated by Wendland kernels with smoothness degree $k \in \mathbb{N}$. Further, let $\mathcal{X} := \bigcup_{i=1}^d \{x_i\} \subset \mathbb{X}$ be a finite set of pairwise-distinct samples and $F \in C^p(\mathbb{X}, \mathbb{R}^n)$, where $p = \lceil \frac{n+1}{2} + k \rceil$, for the right-hand side of system (9). Then, there exist constants $C, h_0 > 0$ such that the following bound on the full approximation error holds for all fill distances $h_{\mathcal{X}} \leq h_0$

$$\|\mathcal{K} - K\|_{\mathbb{H} \rightarrow C^p(\mathbb{X}, \mathbb{R}^n)} \leq Ch_{\mathcal{X}}^{k+1/2}.$$

In conclusion, Theorem 2 states that the kEDMD surrogate K approximates the dynamics (of an autonomous dynamical system) arbitrarily well if only the fill distance $h_{\mathcal{X}}$ is sufficiently small. This result was extended in [14] to control-affine systems

$$x^+ = \hat{F}(x, u) := \hat{g}_0(x) + \sum_{j=1}^m \hat{g}_j(x) u_j \quad (13)$$

with $\hat{g}_j \in \mathcal{C}(\mathbb{R}^n, \mathbb{R}^n)$, $j \in [0 : m]$. We briefly recap the main ingredients analogously to [16].

Data. Let $\mathcal{X} = \{x_1, \dots, x_d\} \subset \mathbb{X}$ be a set of pairwise distinct points, the so-called virtual-observation points with cluster radius $\varepsilon_c > 0$. For each cluster $i \in [1 : d]$, let $d_i \geq m + 1$ data triplets $(x_{ij}, u_{ij}, x_{ij}^+) \in B_{\varepsilon_c}(x_i) \times \mathbb{U} \times \mathbb{R}^n$ satisfying $x_{ij}^+ = \hat{F}(x_{ij}, u_{ij})$ and the condition $\text{rank}([u_{i1} \dots u_{id_i}]) = m$, reminiscent on persistency of excitation as used in [77], on the input data. Then, we approximate the function values $\hat{g}_0(x_i), \dots, \hat{g}_m(x_i)$ in (13) at the virtual observation points $x_i \in \mathcal{X}$ by solving the linear regression problem

$$[\tilde{g}_0(x_i), \tilde{G}(x_i)] = \underset{H \in \mathbb{R}^{n \times (1+m)}}{\text{argmin}} \| [x_{i1}^+ \dots x_{id_i}^+] - HU_i \|_F,$$

where $U_i := \begin{bmatrix} 1 & \dots & 1 \\ u_{i1} & \dots & u_{id_i} \end{bmatrix}$. Due to the imposed rank condition, the unique solution can be expressed using the pseudo-inverse U_i^\dagger .

Interpolating the dynamics. The canonical feature maps $\Phi_{x_i} = k(x_i, \cdot)$ of the Wendland kernels are used to approximately represent the evolution of an observable $\psi : \mathbb{R}^n \rightarrow \mathbb{R}$ under control input u by

$$\psi(x^+) = \sum_{i=1}^d [(\hat{K}_0 \psi_{\mathcal{X}})_i \Phi_{x_i}(x) + \sum_{j=1}^m (\hat{K}_j \psi_{\mathcal{X}})_i \Phi_{x_i}(x) u_j],$$

where we use the notation $\psi_{\mathcal{X}} = (\psi(x_1), \dots, \psi(x_d))^\top$ and $\hat{K}_j = K_{\mathcal{X}}^{-1} K_{\tilde{g}_j} K_{\mathcal{X}}^{-1}$ with $K_{\mathcal{X}} = (k(x_i, x_j))_{i,j=1}^d$ and $K_{\tilde{g}_j} = (k(x_i, \tilde{g}_j(x_i)))_{i=1}^d$ for $j \in [0 : m]$. Choosing the coordinate functions as observables yields a data-driven surrogate for (13) given by

$$x^+ = F^\varepsilon(x, u) := g_0^\varepsilon(x) + \sum_{j=1}^m g_j^\varepsilon(x) u_j,$$

where ε refers to the notation in the following result.

Theorem 3 (Theorem 2 of [16]). For Wendland kernels of smoothness degree $k \geq 1 + \frac{(-1)^n + 1}{2}$, there exist constants $C, h_0, \bar{G}, \bar{U} > 0$ such that for all fill distances $h_{\mathcal{X}} \leq h_0$ the approximation error satisfies for all $(x, u) \in \mathbb{X} \times \mathbb{U}$

$$\|\hat{F}(x, u) - F^\varepsilon(x, u)\|_\infty \leq C(\bar{G} h_{\mathcal{X}}^{k-\frac{1}{2}} \text{dist}(x, \mathcal{X}) + \bar{U} \varepsilon_c),$$

where \bar{G} depends on the approximations $[\tilde{g}_0, \dots, \tilde{g}_m]$, and \bar{U} depends on the input data, the kernel functions and the matrix $K_{\mathcal{X}}^{-1}$, and ε_c is the size of the clusters.

For a detailed representation of the constants we refer to [16, Theorem 2].

Next, we sketch a scheme, in which the safeguarding controller (5) from Section 3 is utilized to ensure a sufficiently-small fill distance $h_{\mathcal{X}}$ and cluster radius ε_c and, thus, a desired guaranteed approximation accuracy by suitably collecting data triplets, cf. the flowchart in Fig. 3. First note that the application of the feedback controller (5) guarantees (3), i.e., output tracking within prescribed bounds on the error $y - y_{\text{ref}}$. To ensure a given fill distance within a subset of the state space $\mathbb{X} \subset \mathbb{R}^{2m}$, we make the following observation: For $x(0) = (y_{\text{ref}}(0), \dot{y}_{\text{ref}}(0))^\top$ and constant error margin $\sigma > 0$, [46, Lem. 2.1] yields for all $t \geq 0$

$$\|e_1(t)\| \leq \frac{\sqrt{5} - 1}{2} =: \delta < 1 \text{ and } \|e_2(t)\| \leq 1.$$

Rewriting the auxiliary variable e_2 in (5), we obtain

$$\|\dot{e}(t)\| = \frac{1}{\sigma} \left\| e_2(t) - \frac{e_1(t)}{1 - \|e_1(t)\|^2} \right\| \leq \frac{1 + \frac{\delta}{1 - \delta^2}}{\sigma} = \frac{2}{\sigma},$$

where $0 < \sigma \in \mathbb{R}_{>0}$ can be chosen (arbitrarily) large. Therefore, invoking $\|y(t) - y_{\text{ref}}(t)\| < 1/\sigma$, we can estimate the error between the state $x(t) \in \mathbb{R}^{2m}$ and the reference and its derivative by

$$\left\| \begin{pmatrix} x_1(t) \\ x_2(t) \end{pmatrix} - \begin{pmatrix} y_{\text{ref}}(t) \\ \dot{y}_{\text{ref}}(t) \end{pmatrix} \right\| < \frac{3}{\sigma}. \quad (14)$$

Based on this line of reasoning, we propose the scheme summarized in Fig. 3 to generate an EDMD-based surrogate model with prescribed approximation error, where the data is collected by steering the system safely through the state space.

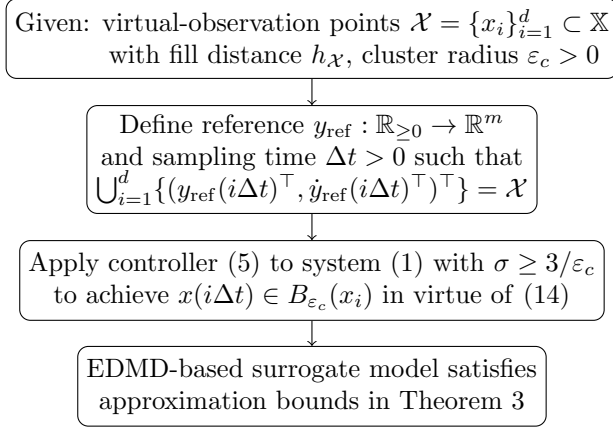


Figure 3: Flowchart illustrating the procedure to generate a data-driven surrogate model with prescribed accuracy using (5)

Note that Fig. 3 is a schematic presentation. In general, the reference will be designed such that for some $D > d$ we have $\bigcup_{i=0}^D \{(y_{\text{ref}}(i\Delta t)^\top, \dot{y}_{\text{ref}}(i\Delta t)^\top)^\top\} \supset \mathcal{X}$. Then, system data is recorded when $x(t) \in B_{\varepsilon_c}$. Moreover, the error margin σ should be chosen such that multiple data points per cluster can be recorded (cf. data requirements after (13)). These aspects are topics of future research. Provided that the details of the above reasoning are formulated precisely, it can then rigorously be ensured that the EDMD-based MPC controller maintains the desired output-tracking specifications using, e.g., the controller design proposed in [70], meaning that the safeguarding mechanism may be switched off.

5 Numerical example

To illustrate the previously presented findings we present a numerical simulation. Consider the nonlinear system

$$\begin{aligned} \dot{x}_1(t) &= x_2(t), \\ \dot{x}_2(t) &= \nu(1 - x_1(t)^2)x_2(t) - x_1(t) + u(t), \end{aligned} \quad (15a)$$

with output

$$y(t) = h(x(t)) = x_1(t), \quad (15b)$$

where $\nu = 0.1$, and $(x_1(0), x_2(0))^\top = (1, -1)^\top \in \mathbb{R}^2$. System (15) is a forced Van-der-Pol oscillator. In this particular example, we have state dimension $n = 2$ and input-output dimension $m = 1$. System (15) satisfies the structural Assumption 1, and hence belongs to the system class specified in Section 2.1. According to Assumption 2 we have access to the signals $y(t)$ and $\dot{y}(t)$. We choose the following set of observables

$$\Psi = \{x_1^p \cdot x_2^q \mid p, q \in \{0, 1, 2, 3\}, p + q \leq 3\},$$

meaning that we have 10 observables consisting of all monomials of the state up to degree 3. In particular, the

coordinate functions are contained. For the cost function in Algorithm 1 we choose the weighting matrices $Q = \text{diag}(10^4, 1) \in \mathbb{R}^{2 \times 2}$ and $R = 10^{-4}$. We choose the prediction horizon to be $N = 30$, and constrain the prediction-based input by $\|\mu(\cdot)\| \leq 2$, i.e., $\mathbb{U} = [-2, 2]$. The sampling time for EDMD is set to $\Delta t = 0.05$. For the activation function $a_\tau(\cdot)$ in (6) we choose $\lambda = 0.75$ as activation threshold, and $\tau = \Delta t/2$ as dwell-time.

We consider two control tasks. First we aim to stabilize the system to the origin; second, we perform a set-point transition. For both tasks we choose the funnel function

$$\sigma(t) = \begin{cases} \frac{1}{2.3} & t \leq 4, \\ \frac{1}{2e^{-2(t-4)} + 0.3} & t > 4, \end{cases} \quad (16)$$

which allows a larger error at the beginning, cf. Figs. 4 and 6. This prevents early intervention of the safeguard and allows for data collection during tracking.

5.1 Stabilization

First, we simulate stabilization of (15), i.e., $y_{\text{ref}}(t) \equiv 0$ for all $t \geq 0$. We consider the following situation. We assume that we have access to $d = 10$ data points (e.g. from previous experiments) collected in $\mathbb{X} = [2, 2]^2$ with sampling time $\Delta t = 0.05$, i.e., we start with *some* approximation of the Koopman operator. To improve the model, we collect data whenever $a_\tau(t, e_2(t)) = 0$ for all $t \in [k\Delta t, (k+1)\Delta t)$ and alternately apply $\mu(t) = 1$ and $\mu(t) = 0$, until $d = 25$ (cf. Remark 3). The con-

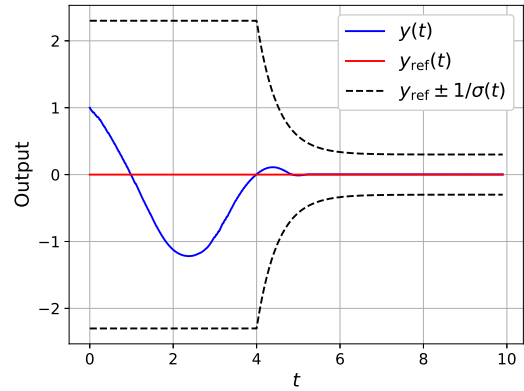


Figure 4: Stabilizing the origin. Visualization of the output $y(t) = x_1(t)$ and the error boundary $\sigma(t)$ given by (16).

trol input $u(\cdot)$ and activation function $a_\tau(\cdot)$ are depicted in Fig. 5. It can be seen that at some point in the exploration phase the safeguarding funnel controller intervenes. After some time the approximation of the Koopman operator sufficiently well represents the dynamics and the tracking task is performed with purely data-based predictions.

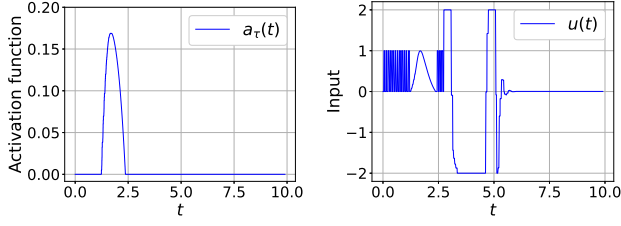


Figure 5: Stabilizing the origin. Visualization of the activation function $a_\tau(t, e_2(t))$ (left) and the input $u(t) = \mu(t) + a_\tau(t, e_2(t)) u_{\text{FC}}(t)$ (right).

5.2 Set-point transition

As a second scenario we consider transition between two set-points. To ensure $y_{\text{ref}} \in W^{2,\infty}([0, \infty), \mathbb{R}^2)$, we connect the two set-points with a smooth function. We define the overall reference trajectory by

$$y_{\text{ref}}^{\bar{t}}(t) = 1 + \frac{2}{\pi} \int_0^t e^{-(s-\bar{t})^2} ds,$$

parameterized by the shift \hat{t} . Note that $y_{\text{ref}} \approx 0$ at the beginning, and $y_{\text{ref}} \approx 2$ in the end.

5.2.1 Initializing with ten i.i.d. data points

First we consider the situation when the model is initialized with 10 i.i.d. generated data points. We choose the reference y_{ref}^{10} . Accordingly, the results look similar to the previous simulation at the beginning.

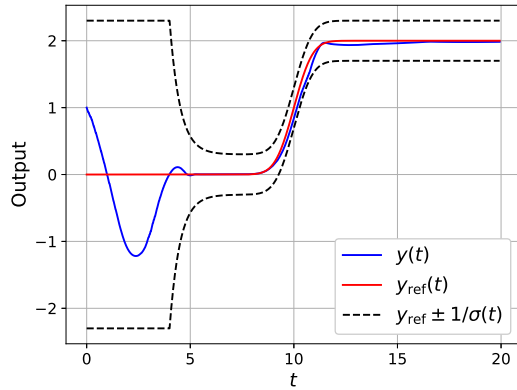


Figure 6: Set-point transition. Visualization of the output $y(t) = x_1(t)$, reference and error boundary $1/\sigma(t)$.

In the transition phase maintaining the output constraints is challenging, see Fig. 7, where the funnel controller is activated three times ($a_\tau \neq 0$) and intervenes the predictive control. However, the error bounds are guaranteed, see Fig. 6. After the transition phase the EDMD-based MPC is again capable of keeping the system close to the set-point, which is a controlled equilibrium matching the input constraints.

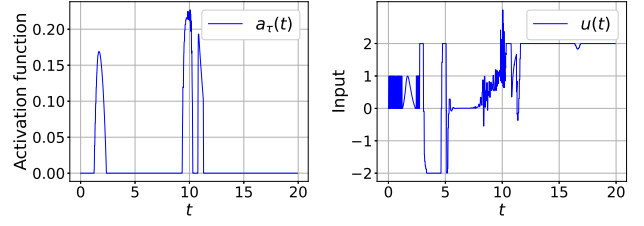


Figure 7: Set-point transition. Visualization of the activation function $a_\tau(t, e_2(t))$ (left) and control input.

5.2.2 Initializing with one data point

Next, we start with only one data point and collect data on runtime (the one data point is used to initialize the algorithm). To account for the lack of data, we start with a larger funnel and choose the reference y_{ref}^{16} , i.e., we allow the system to evolve “freely” for a longer period, see Fig. 8. For simulation purpose we limit the data to $d = 100$. Similarly to the previous scenario, the

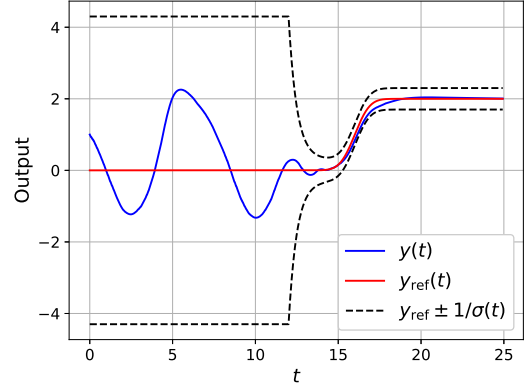


Figure 8: Set-point transition, initializing with 1 data point. Visualization of the output $y(t) = x_1(t)$, reference and error boundary $1/\sigma(t)$.

funnel controller intervenes three times in the transition phase due to the tight error margin, cf. Fig. 9. After the learning process the data-based MPC is capable of keeping the system at the controlled equilibrium. How-

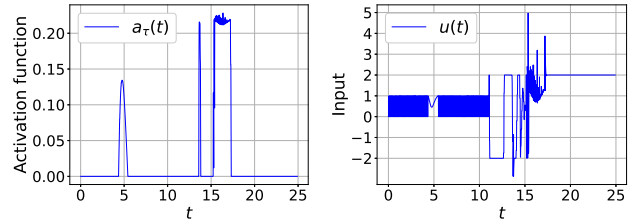


Figure 9: Set-point transition, initializing with 1 data point. Visualization of the activation function $a_\tau(t, e_2(t))$ (left) and control input (right).

ever, while the error bounds are still maintained during the set-point change, using this data sampling process, leads to control values, that distinctly exceed the input constraints for the MPC.

6 Conclusions and outlook

We have proposed a two-component controller design for nonlinear control systems to achieve safe data-driven predictive tracking control. The data-driven component has been exemplified by DeePC and EDMD. Two scenarios have been considered. First, the reactive model-free feedback controller safeguards the tracking with DeePC and EDMD-based MPC. Second, using the guarantees from the feedback can be utilized to achieve a certain sampling quality (fill distance). The proposed two-component controller (4) is open to many extensions and modifications such as updating the data matrices and deleting old data (shifting the sampling window); starting the control task with a small prediction horizon and depending on the amount of data, the prediction horizon is gradually increased (as done for DeePC in [68]); or use only few data (cf. model order reduction), which results in small data matrices and hence saves computation time. Depending on the application, these ideas can be selected and combined while maintaining the guarantees for the tracking error. In future work we will thoroughly analyze the scheme proposed in Section 4.2.3 to, e.g., formulate requirements on the data and the reference defined through the virtual-observation points.

Acknowledgment. L. Bold and L. Lanza gratefully acknowledge funding by the German Research Foundation DFG (Project-ID 471539468 and 545246093; Deutsche Forschungsgemeinschaft) and by the Carl Zeiss Foundation (Project-ID 2011640173; VerneDCt).

References

- [1] Mohammad Alsalti, Julian Berberich, Victor G Lopez, Frank Allgöwer, and Matthias A Müller. “Data-based system analysis and control of flat nonlinear systems”. In: *60th IEEE Conference on Decision and Control (CDC)*. 2021.
- [2] Aaron D Ames, Samuel Coogan, Magnus Egerstedt, Gennaro Notomista, Koushil Sreenath, and Paulo Tabuada. “Control barrier functions: Theory and applications”. In: *18th European control conference (ECC)*. 2019.
- [3] Mituhiko Araki and Hidefumi Taguchi. “Two-degree-of-freedom PID controllers”. In: *International Journal of Control, Automation, and Systems* 1.4 (2003).
- [4] H Harry Asada and Jose A Solano-Castellanos. “Control-Coherent Koopman Modeling: A Physical Modeling Approach”. In: *arXiv preprint arXiv:2403.16306* (2024).
- [5] Anil Aswani, Humberto Gonzalez, S Shankar Sastry, and Claire Tomlin. “Provably safe and robust learning-based model predictive control”. In: *Automatica* 49.5 (2013).
- [6] Guaraci Bastos Jr, Robert Seifried, and Olivier Brüls. “Analysis of stable model inversion methods for constrained underactuated mechanical systems”. In: *Mechanism and Machine Theory* 111 (2017).
- [7] Charalampos P Bechlioulis and George A Rovithakis. “A low-complexity global approximation-free control scheme with prescribed performance for unknown pure feedback systems”. In: *Automatica* 50.4 (2014).
- [8] Charalampos P Bechlioulis and George A Rovithakis. “Prescribed performance adaptive control for multi-input multi-output affine in the control nonlinear systems”. In: *IEEE Transactions on automatic control* 55.5 (2010).
- [9] Thomas Berger, Dario Dennstädt, Lukas Lanza, and Karl Worthmann. “Robust Funnel Model Predictive Control for output tracking with prescribed performance”. In: *SIAM Journal on Control and Optimization* 62.4 (2024).
- [10] Thomas Berger, Achim Ilchmann, and Eugene P Ryan. “Funnel control of nonlinear systems”. In: *Mathematics of Control, Signals, and Systems* 33 (2021).
- [11] Dimitri Bertsekas. *Reinforcement learning and optimal control*. Vol. 1. Athena Scientific, 2019.
- [12] Andrea Boccia, Lars Grüne, and Karl Worthmann. “Stability and feasibility of state constrained MPC without stabilizing terminal constraints”. In: *Systems & control letters* 72 (2014).
- [13] Lea Bold, Lars Grüne, Manuel Schaller, and Karl Worthmann. “Data-driven MPC with stability guarantees using extended dynamic mode decomposition”. In: *IEEE Transactions on Automatic Control* (2024).
- [14] Lea Bold, Friedrich M Philipp, Manuel Schaller, and Karl Worthmann. “Kernel-based Koopman approximants for control: Flexible sampling, error analysis, and stability”. In: *Preprint arXiv:2412.02811* (2024).
- [15] Lea Bold, Mario Rosenfelder, Hannes Eschmann, Henrik Ebel, and Karl Worthmann. “On Koopman-based surrogate models for non-holonomic robots”. In: *IFAC-PapersOnLine* 58.21 (2024).

- [16] Lea Bold, Manuel Schaller, Irene Schimperna, and Karl Worthmann. “Kernel EDMD for data-driven nonlinear Koopman MPC with stability guarantees”. In: *Preprint arxiv:2501.08709* (2025).
- [17] Daniel Bruder, Xun Fu, and Ram Vasudevan. “Advantages of bilinear Koopman realizations for the modeling and control of systems with unknown dynamics”. In: *IEEE Robotics and Automation Letters* 6.3 (2021).
- [18] Steven L Brunton, Bingni W Brunton, Joshua L Proctor, and J Nathan Kutz. “Koopman invariant subspaces and finite linear representations of nonlinear dynamical systems for control”. In: *PloS one* 11.2 (2016).
- [19] Steven L Brunton, Marko Budišić, Eurika Kaiser, and J Nathan Kutz. “Modern Koopman theory for dynamical systems”. In: *SIAM Review* 64.2 (2022).
- [20] Mo Chen and Claire J Tomlin. “Hamilton–jacobi reachability: Some recent theoretical advances and applications in unmanned airspace management”. In: *Annual Review of Control, Robotics, and Autonomous Systems* 1.1 (2018).
- [21] Jeremy Coulson, John Lygeros, and Florian Dörfler. “Data-enabled predictive control: In the shallows of the DeePC”. In: *18th European Control Conference (ECC)*. 2019.
- [22] Claudio De Persis and Pietro Tesi. “Formulas for data-driven control: Stabilization, optimality, and robustness”. In: *IEEE Transactions on Automatic Control* 65.3 (2019).
- [23] Claudio De Persis and Pietro Tesi. “Learning controllers for nonlinear systems from data”. In: *Annual Reviews in Control* 56.100915 (2023).
- [24] Florian Dörfler, Jeremy Coulson, and Ivan Markovsky. “Bridging direct and indirect data-driven control formulations via regularizations and relaxations”. In: *IEEE Transactions on Automatic Control* 68.2 (2022).
- [25] Svenja Drücker, Lukas Lanza, Thomas Berger, Timo Reis, and Robert Seifried. “Experimental validation for the combination of funnel control with a feedforward control strategy”. In: *Multibody System Dynamics* (2024).
- [26] Timm Faulwasser, Ruchuan Ou, Guanru Pan, Philipp Schmitz, and Karl Worthmann. “Behavioral theory for stochastic systems? A data-driven journey from Willems to Wiener and back again”. In: *Annual Reviews in Control* 55 (2023).
- [27] Carl Folkestad and Joel W Burdick. “Koopman NMPC: Koopman-based learning and nonlinear model predictive control of control-affine systems”. In: *IEEE International Conference on Robotics and Automation (ICRA)*. 2021.
- [28] Javier Garcia and Fernando Fernández. “A comprehensive survey on safe reinforcement learning”. In: *Journal of Machine Learning Research* 16.1 (2015).
- [29] Pieter van Goor, Robert Mahony, Manuel Schaller, and Karl Worthmann. “Reprojection methods for Koopman-based modelling and prediction”. In: *62nd IEEE Conference on Decision and Control (CDC)*. 2023.
- [30] Debdipta Goswami and Derek A. Paley. “Bilinearization, reachability, and optimal control of control-affine nonlinear systems: A Koopman spectral approach”. In: *IEEE Transactions on Automatic Control* 67.6 (2021).
- [31] Simon Gottschalk, Lukas Lanza, Karl Worthmann, and Kerstin Lux-Gottschalk. “Reinforcement Learning for Docking Maneuvers with Prescribed Performance”. In: *IFAC-PapersOnLine* 58.17 (2024).
- [32] Lars Grüne, Jürgen Pannek, Martin Seehafer, and Karl Worthmann. “Analysis of unconstrained nonlinear MPC schemes with time varying control horizon”. In: *SIAM Journal on Control and Optimization* 48.8 (2010).
- [33] Lukas Hewing, Kim P Wabersich, Marcel Menner, and Melanie N Zeilinger. “Learning-based model predictive control: Toward safe learning in control”. In: *Annual Review of Control, Robotics, and Autonomous Systems* 3.1 (2020).
- [34] Lucian Cristian Iacob, Roland Tóth, and Maarten Schoukens. “Koopman form of nonlinear systems with inputs”. In: *Automatica* 162 (2024).
- [35] Achim Ilchmann, Eugene P Ryan, and Christopher J. Sangwin. “Tracking with prescribed transient behaviour”. In: *ESAIM: Control, Optimisation and Calculus of Variations* 7 (2002).
- [36] Tobias Johannink, Shikhar Bahl, Ashvin Nair, Jianlan Luo, Avinash Kumar, Matthias Loskyll, Juan Aparicio Ojea, Eugen Solowjow, and Sergey Levine. “Residual reinforcement learning for robot control”. In: *IEEE International Conference on Robotics and Automation (ICRA)*. 2019.
- [37] Bahare Kiumarsi, Kyriakos G Vamvoudakis, Hamidreza Modares, and Frank L Lewis. “Optimal and autonomous control using reinforcement learning: A survey”. In: *IEEE Transactions on Neural Networks and Learning Systems* 29.6 (2017).
- [38] Stefan Klus, Feliks Nüske, and Boumediene Hamzi. “Kernel-based approximation of the Koopman generator and Schrödinger operator”. In: *Entropy* 22.7 (2020).

- [39] Stefan Klus, Feliks Nüske, Sebastian Peitz, Jan-Hendrik Niemann, Cecilia Clementi, and Christof Schütte. “Data-driven approximation of the Koopman generator: Model reduction, system identification, and control”. In: *Physica D: Nonlinear Phenomena* 406.132416 (2020).
- [40] Frederik Köhne, Friedrich M Philipp, Manuel Schaller, Anton Schiela, and Karl Worthmann. “ L^∞ -error bounds for approximations of the Koopman operator by kernel extended dynamic mode decomposition”. In: *SIAM Journal on Applied Dynamical Systems* (2024). To appear (arXiv preprint arXiv:2403.18809).
- [41] Bernard O Koopman. “Hamiltonian systems and transformation in Hilbert space”. In: *Proceedings of the National Academy of Sciences* 17.5 (1931).
- [42] Bernard O Koopman and John von Neumann. “Dynamical systems of continuous spectra”. In: *Proceedings of the National Academy of Sciences* 18.3 (1932).
- [43] Milan Korda and Igor Mezić. “Linear predictors for nonlinear dynamical systems: Koopman operator meets model predictive control”. In: *Automatica* 93 (2018).
- [44] Milan Korda and Igor Mezić. “On convergence of extended dynamic mode decomposition to the Koopman operator”. In: *Journal of Nonlinear Science* 28.2 (2018).
- [45] Milan Korda and Igor Mezić. “Optimal construction of Koopman eigenfunctions for prediction and control”. In: *IEEE Transactions on Automatic Control* 65.12 (2020).
- [46] Lukas Lanza, Dario Dennstädt, Karl Worthmann, Philipp Schmitz, Gökçen Devlet Şen, Stephan Trenn, and Manuel Schaller. “Sampled-data funnel control and its use for safe continual learning”. In: *Systems & Control Letters* 192.105892 (2024).
- [47] Tengfei Liu and Zhong-Ping Jiang. “Event-based control of nonlinear systems with partial state and output feedback”. In: *Automatica* 53 (2015).
- [48] Jan Lunze and Daniel Lehmann. “A state-feedback approach to event-based control”. In: *Automatica* 46.1 (2010).
- [49] Tim Martin and Frank Allgöwer. “Data-Driven System Analysis of Nonlinear Systems Using Polynomial Approximation”. In: *IEEE Transactions on Automatic Control* 69.7 (2024).
- [50] Alexandre Mauroy and Jorge Goncalves. “Koopman-based lifting techniques for nonlinear systems identification”. In: *IEEE Transactions on Automatic Control* 65.6 (2019).
- [51] Alexandre Mauroy and Jorge Goncalves. “Linear identification of nonlinear systems: A lifting technique based on the Koopman operator”. In: *55th IEEE Conference on Decision and Control (CDC)*. 2016.
- [52] Alexandre Mauroy, Y Susuki, and Igor Mezić. *Koopman operator in systems and control*. Springer, 2020.
- [53] Igor Mezić. “Analysis of fluid flows via spectral properties of the Koopman operator”. In: *Annual review of fluid mechanics* 45 (2013).
- [54] Igor Mezić. “On numerical approximations of the Koopman operator”. In: *Mathematics* 10.7 (2022).
- [55] Igor Mezić. “Spectral properties of dynamical systems, model reduction and decompositions”. In: *Nonlinear Dynamics* 41.1-3 (2005).
- [56] Abhinav Narasingam, Sang Hwan Son, and Joseph Sang-Il Kwon. “Data-driven feedback stabilisation of nonlinear systems: Koopman-based model predictive control”. In: *International Journal of Control* 96.3 (2023).
- [57] Feliks Nüske, Sebastian Peitz, Friedrich Philipp, Manuel Schaller, and Karl Worthmann. “Finite-data error bounds for Koopman-based prediction and control”. In: *Journal of Nonlinear Science* 33.14 (2023).
- [58] Matthew Osborne, Hyo-Sang Shin, and Antonios Tsourdos. “A review of safe online learning for nonlinear control systems”. In: *International Conference on Unmanned Aircraft Systems (ICUAS)*. 2021.
- [59] Sebastian Peitz, Samuel E Otto, and Clarence W Rowley. “Data-driven model predictive control using interpolated Koopman generators”. In: *SIAM Journal on Applied Dynamical Systems* 19.3 (2020).
- [60] Theodore J Perkins and Andrew G Barto. “Lyapunov design for safe reinforcement learning”. In: *Journal of Machine Learning Research* 3 (2002).
- [61] Friedrich M Philipp, Manuel Schaller, Septimus Boshoff, Sebastian Peitz, Feliks Nüske, and Karl Worthmann. “Variance representations and convergence rates for data-driven approximations of Koopman operators”. In: *ArXiv preprint arXiv:2402.02494* (2024).
- [62] Friedrich M Philipp, Manuel Schaller, Karl Worthmann, Sebastian Peitz, and Feliks Nüske. “Error bounds for kernel-based approximations of the Koopman operator”. In: *Applied and Computational Harmonic Analysis* 71.101657 (2024).

- [63] Joshua L Proctor, Steven L Brunton, and J Nathan Kutz. “Dynamic mode decomposition with control”. In: *SIAM Journal on Applied Dynamical Systems* 15.1 (2016).
- [64] Daniel E Quevedo, Vijay Gupta, Wann-Jiun Ma, and Serdar Yüksel. “Stochastic stability of event-triggered anytime control”. In: *IEEE Transactions on Automatic Control* 59.12 (2014).
- [65] Mario Rosenfelder, Lea Bold, Hannes Eschmann, Peter Eberhard, Karl Worthmann, and Henrik Ebel. “Data-Driven Predictive Control of Nonholonomic Robots Based on a Bilinear Koopman Realization: Data Does Not Replace Geometry”. In: *arXiv preprint arXiv:2411.07192* (2024).
- [66] J Sánchez, Antonio Visioli, and S Dormido. “A two-degree-of-freedom PI controller based on events”. In: *Journal of Process Control* 21.4 (2011).
- [67] Philipp Schmitz, Timm Faulwasser, Paolo Rapisarda, and Karl Worthmann. “A continuous-time fundamental lemma and its application in data-driven optimal control”. In: *Systems & Control Letters* 194.105950 (2024).
- [68] Philipp Schmitz, Lukas Lanza, and Karl Worthmann. “Safe data-driven reference tracking with prescribed performance”. In: *27th International Conference on System Theory, Control and Computing (ICSTCC)*. IEEE. 2023.
- [69] Sigurd Skogestad and Ian Postlethwaite. *Multivariable feedback control: analysis and design*. John Wiley & Sons, 2005.
- [70] Raffaele Soloperto, Johannes Köhler, and Frank Allgöwer. “A nonlinear MPC scheme for output tracking without terminal ingredients”. In: *IEEE Transactions on Automatic Control* 68.4 (2022).
- [71] Robin Strässer, Manuel Schaller, Karl Worthmann, Julian Berberich, and Frank Allgöwer. “Koopman-based feedback design with stability guarantees”. In: *IEEE Transactions on Automatic Control* (2024).
- [72] Amit Surana. “Koopman operator based observer synthesis for control-affine nonlinear systems”. In: *55th IEEE Conference on Decision and Control (CDC)*. 2016.
- [73] Chris Verhoek, Roland Tóth, Sofie Haesaert, and Anne Koch. “Fundamental lemma for data-driven analysis of linear parameter-varying systems”. In: *60th IEEE conference on decision and control (CDC)*. 2021.
- [74] Kim P Wabersich and Melanie N Zeilinger. “A predictive safety filter for learning-based control of constrained nonlinear dynamical systems”. In: *Automatica* 129.109597 (2021).
- [75] Kim P Wabersich and Melanie N Zeilinger. “Predictive control barrier functions: Enhanced safety mechanisms for learning-based control”. In: *IEEE Transactions on Automatic Control* 68.5 (2022).
- [76] Holger Wendland. *Scattered data approximation*. Vol. 17. Cambridge university press, 2004.
- [77] Jan C Willems, Paolo Rapisarda, Ivan Markovsky, and Bart LM De Moor. “A note on persistency of excitation”. In: *Systems & Control Letters* 54.4 (2005).
- [78] Matthew Williams, Ioannis Kevrekidis, and Clarence Rowley. “A Data-Driven Approximation of the Koopman Operator: Extending Dynamic Mode Decomposition”. In: *Journal of Nonlinear Science* 25.6 (2015).
- [79] Matthew O Williams, Clarence W Rowley, and Ioannis G Kevrekidis. “A kernel-based method for data-driven koopman spectral analysis”. In: *Journal of Computational Dynamics* 2.2 (2016).
- [80] Christophe Zhang and Enrique Zuazua. “A quantitative analysis of Koopman operator methods for system identification and predictions”. In: *Comptes Rendus. Mécanique* 351.S1 (2023).